Accepted Manuscript

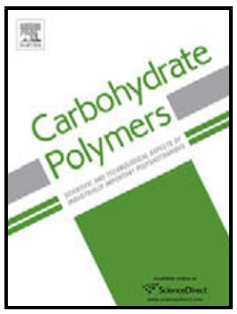

Title: Extracellular depolymerisation triggers fermentation of tamarind xyloglucan and wheat arabinoxylan by a porcine faecal inoculum

Authors: Guangli Feng, Bernadine M. Flanagan, Barbara A. Williams, Deirdre Mikkelsen, Wenwen Yu, Michael J. Gidley

PII: S0144-8617(18)30997-4
DOI: https://doi.org/10.1016/j.carbpol.2018.08.089
Reference: CARP 13986

To appear in:

Received date: 7-6-2018
Revised date: 20-8-2018
Accepted date: 20-8-2018

Please cite this article as: Feng G, Flanagan BM, Williams BA, Mikkelsen D, Yu W, Gidley MJ, Extracellular depolymerisation triggers fermentation of tamarind xyloglucan and wheat arabinoxylan by a porcine faecal inoculum, *Carbohydrate Polymers* (2018), https://doi.org/10.1016/j.carbpol.2018.08.089

Title: Extracellular depolymerisation triggers fermentation of tamarind xyloglucan and wheat arabinoxylan by a porcine faecal inoculum

Guangli Feng[a], Bernadine M. Flanagan[a], Barbara A. Williams[a], Deirdre Mikkelsen[a], Wenwen Yu[b] & Michael J. Gidley[a,*]

[a] ARC Centre of Excellence in Plant Cell Walls, Centre for Nutrition and Food Sciences, Queensland Alliance for Agriculture and Food Innovation, The University of Queensland, St Lucia, QLD, Australia 4072.

[b] Centre for Nutrition and Food Sciences, Queensland Alliance for Agriculture and Food Innovation, The University of Queensland, St Lucia, QLD, Australia 4072.

Guangli Feng: g.feng@uq.edu.au

Bernadine M. Flanagan: b.flanagan@uq.edu.au

Barbara A. Williams: b.williams@uq.edu.au

Deirdre Mikkelsen: d.mikkelsen@uq.edu.au

Wenwen Yu: w.yu1@uq.edu.au

*Michael J. Gidley: m.gidley@uq.edu.au; Tel: +6173365 2145; Fax: +61733651188; Address: Room C408, Hartley Teakle Building [#83], The University of Queensland, St Lucia, 4072.

Highlights

- Depolymerisation on microbial surfaces initiates fermentation of XG/AX by porcine faeces
- Depolymerised XG/AX released back into medium suggesting cross-feeding
- Acetate and propionate produced at the same time as XG/AX degradation
- Butyrate and gas production occur later than XG/AX degradation

Abstract:

Arabinoxylan (AX) and xyloglucan (XG) are important components of primary cell walls of cereal grains and vegetables/fruits, respectively. Despite the established health benefits of these non-starch polysaccharides, the mechanisms of their utilisation by the gut microbiota are poorly understood. In this study, the mechanisms of solubilised wheat AX and tamarind XG degradation were investigated under *in vitro* fermentation conditions using a porcine faecal inoculum. Through structural analysis of the polymers, we

demonstrate that depolymerisation by microbial surface accessible *endo*-degrading enzymes occurs prior to active fermentation of AX or XG. Breakdown products are released into the medium and potentially utilised cooperatively by other microbes. Acetate and propionate are the main fermentation products and are produced concurrently with polysaccharide depletion. Butyrate, however, is produced more slowly consistent with it being a secondary metabolite.

Key words: Xyloglucan; Arabinoxylan; *In vitro* fermentation; Short chain fatty acid; Gut microbiota

1 Introduction

Plant cell walls are rich in polysaccharides and are the main structural components of plant-based foods such as grains, fruits and vegetables. They are not digested or absorbed in the human small intestine, and therefore pass to the large intestine where they are available for fermentation by the resident microbiota (Gidley, 2013; Harris & Smith, 2006; Mikkelsen, Gidley, & Williams, 2011). The fermentation of these polymers is not only critical in maintaining colonic health (Neyrinck et al., 2011), but also has profound effects on host metabolism, and the immune system (Mendis, Leclerc, & Simsek, 2016).

Xyloglucan (XG) is found in the cell walls of almost all land plants. It is abundant in the primary walls of vegetables and fruits (Larsbrink, Rogers, et al., 2014), as well as in the seeds of some species, e.g. tamarind, as a storage polymer providing energy for germination (Schultink, Liu, Zhu, & Pauly, 2014). The structure of XG consists of a β-1,4-glucopyranose (Glc*p*) backbone partially substituted with α-D-xylopyranose (α-D-Xyl*p*) at C(O)6. The α-D-Xyl*p* residues can be further substituted with other monosaccharides, including galactose (such as in tamarind seed), fucose (such as in eudicotyledons) and/or arabinose (such as in Solanaceae) (Hsieh & Harris, 2009). The structure of tamarind XG (**Figure 1**) consists of four motifs, a heptasaccharide (XXXG, Glc_4Xyl_3), two octasaccharides (XXLG and XLXG, Glc_4Xyl_3Gal) and a nonasaccharide (XLLG, $Glc_4Xyl_3Gal_2$), with the ratio of hepta-/octa-/nona-saccharide being 13:39:48 (Yamatoya, Shirakawa, Kuwano, Suzuki, & Mitamura, 1996).

Arabinoxylan (AX) is especially abundant in the primary cell walls of many cereal grains. The backbone of wheat or rye AX consists of β-(1,4)-linked D-xylopyranosyl units which are doubly substituted with arabinofuranosyl moieties at C(O)2 and C(O)3 ($A^{2+3}X$), or singly substituted at C(O)3 (A^3X) (**Figure 1**).

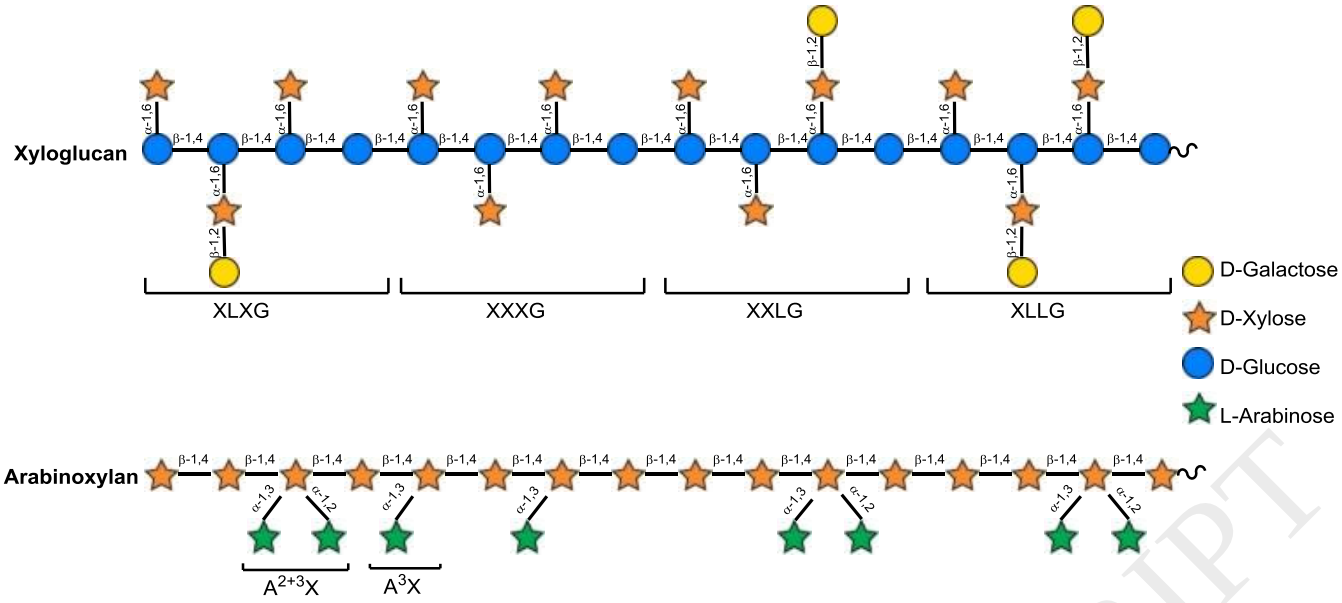

Figure 1 Structural features present in tamarind xyloglucan and wheat arabinoxylan. Note that the sequence of these features is not defined.

The large intestinal microbiota produce various enzymes which degrade XG/AX into their monosaccharide components, which are then metabolised into smaller molecules, such as short chain fatty acids (SCFA) (Larsbrink, Rogers, et al., 2014; Rogowski et al., 2015). The complete degradation of XG into monosaccharides (glucose, xylose and galactose in the case of tamarind XG) requires the concerted action of *endo*-β-1,4-xyloglucanase, *exo*-β-glucosidase, *exo*-α-xylosidase and *exo*-β-galactosidase. Similarly, to degrade AX into xylose and arabinose, *endo*-β-xylanase, *exo*-α-arabinofuranosidases and *exo*-β-xylosidase are needed. Genomic and metagenomic analyses identify both extracellular and intracellular XG/AX-degrading enzymes, and putative degradation pathways within single microbes have been proposed (Larsbrink, Rogers, et al., 2014; Ravachol et al., 2016; Rogowski et al., 2015). However, systems using single microbes are limited, as the gut microbiota contains hundreds of microbial species in a highly dynamic and competitive gut environment. Therefore, it is useful to include the entire microbial community to understand how specific polysaccharides are degraded.

In our previous study, general features of AX utilisation by a porcine faecal inoculum were deduced using AX in a powdered state (Feng et al., 2018). However, when powdered XG was used, gel lumps were apparent in the medium, which inhibited utilisation by the microbes to a variable extent. Therefore, in order to examine the mechanisms of XG utilisation, XG was pre-dissolved. Pre-dissolved AX was also included in this study to compare with powdered AX. A porcine faecal inoculum was used as a model for colonic microbiota (Miller & Ullrey, 1987; Roura et al., 2016), and a semi-defined medium was used in which the XG/AX polymers were the only carbon sources available for energy. AX and XG are large polymers and are not expected to be able to pass through the microbial cell walls (Demchick & Koch, 1995). Therefore, the hypothesis was that both XG and AX in solution would be depolymerised and debranched by microbial surface-accessible enzymes with release of degradation products back into the medium during active fermentation.

2 Materials and methods

2.1 Materials

XG (product code: P-XYGLN) and AX (product code: P-WAXYM) were purchased from Megazyme (Bray, Ireland). Dimethyl sulfoxide-d_6 (DMSO-d_6, 99.9 atom % D, 151874), deuterium oxide (D_2O, 99.9 atom % D, 151882) and 3-(trimethylsily) propionic-2,2,3,3-d_4 acid sodium salt (TSP, 98 atom % D, 269913) were purchased from Sigma-Aldrich (Castle Hill, Australia).

2.2 *In vitro* fermentation of XG and AX

2.2.1 Preparation of the substrate solutions

For each polymer, XG or AX, 21 g was dissolved overnight at 25 ^{o}C in boiled Milli-Q water (2.1 L) with constant stirring and bubbling with a stream of oxygen-free carbon dioxide, and then dispensed into serum bottles (38 mL). The bottles were sealed with butyl rubber stoppers, aluminium caps crimped, and autoclaved (15 min, 121 °C).

2.2.2 Preparation of the medium

The medium was modified from Lowe *et al.* (Lowe, Theodorou, Trinci, & Hespell, 1985) and Williams *et al.* (Williams, Bosch, Boer, Verstegen, & Tamminga, 2005). In brief, the concentration of the 'basal solution' was double that of the basal solution described by Williams *et al.* (Williams et al., 2005), and each serum bottle contained 38 mL of the concentrated basal solution. The basal solution contained 1.189 g/L trypticase as a source of peptides and amino acids, as well as 0.642 g/L NH_4Cl as an addition source of nitrogen in the form of ammonium. The vitamin/phosphate solution, bicarbonate solution, and reducing agent were prepared according to methods described by Williams *et al.* (Williams et al., 2005).

2.2.3 Preparation of the inoculum

The inoculum was prepared based on the method described by Williams *et al.* (Williams et al., 2005). Faeces were collected from five pigs fed on a standard semi-defined diet for ten days prior to collection. The diet, based on readily digestible maize starch and fishmeal (Feng et al., 2018), was formulated to be as free as possible of XG or AX to avoid adaptation of the microbiota. The faeces were diluted five times (w/v) with pre-warmed (39 °C), sterile, saline solution (9 g/L NaCl). The inoculum was obtained after homogenisation of the faeces with a hand mixer for 60s, and filtration through four layers of muslin cloth.

2.2.4 Fermentation

The 'substrate solution' and the 'basal solution' were combined under a constant flow of CO_2. Then, 1 mL of the 'vitamin/phosphate solution', 4 mL of the 'bicarbonate solution' and 1 mL of the 'reducing agent' were added (Williams et al., 2005). Following inoculation, fermentation proceeded for up to 72 h at 39 °C. Two blanks were included. One blank contained the substrate and the medium but the inoculum was substituted by 5 ml saline solution (AX_Med or XG_Med), for which there were two replicates each at 0 h and at 72 h. The other blank contained the medium and the inoculum but no substrates (Inoc_Med, 38 mL of

autoclaved Millipore water was used), for which two bottles were taken for each time removal point (0 h, 2 h, 4 h, 6 h, 8 h, 10 h, 12 h, 18 h, 24 h, 48 h, and 72 h).

At each time removal point, the microbial activity was retarded by plunging the bottles into ice water for 20 min, and samples were taken for various analyses according to the methods described by Feng *et al* (Feng et al., 2018).

2.2.5 Cumulative gas production

Cumulative gas production was calculated according to the method described by Williams *et al.* (Williams et al., 2005). In brief, at regular time intervals, the fermentation bottles were connected to a pressure transducer and the pressure inside the bottles was recorded. Gas was removed manually using a syringe until the pressure returned to baseline, and the volume of gas was recorded. The gas volume was latter corrected according to the regression of recorded pressure and volume. The corrected volume at each time per bottle was cumulated to calculate the cumulative gas production.

2.3 Short chain fatty acids (SCFA) and ammonia (NH_3) analyses

At the end of fermentation, samples of the top phase liquid were collected for SCFA and ammonia analyses, for which samples were stabilised with 20% metaphosphoric acid and 0.2 M HCl, respectively.

SCFA were analysed using modified methods from Williams *et al.* (Williams, Mikkelsen, Le Paih, & Gidley, 2011). A gas chromatograph (Shimadzu GC-2010, Kyoto, Japan) connected with an AOC-20i auto injector (Kyoto, Japan), a flame ionization detector (FID) and a ZB-FFAP column (30 m × 0.53 mm, J & W Scientific, USA) was used. The temperatures for the injector, detector and column were 180 °C, 210 °C and 85 °C respectively. Initially, the temperature was 85 °C for 4 min, then increased to 200 °C at a rate of 15 °C/min. The branched-chain percentage (BCP) was the mole percentage of branched-chain SCFA (*iso*-butyrate, *iso*-valerate) and valerate to the total SCFA.

Ammonia was determined according to the method first described by Baethgen and Alley (Baethgen & Alley, 1989), as modified by Williams *et al.* (Williams et al., 2005). In brief, after stabilisation with equal volume of 0.1 M HCl, ammonia was determined using sodium hypochlorite and sodium nitroprusside at 623 nm.

2.4 Enzymatic hydrolysis of XG and AX with the inoculum supernatant

The prepared inoculum (described in **2.2.3**) was centrifuged for 20 min at 14,000 g and 4 °C. The supernatant was filtered through 0.22 μm filters to ensure complete removal of the microbes. Then 2.5 mL of this filtrate was added into serum bottles containing half the volume of the complete medium and the substrates (see **2.2**). The mixture was incubated at 39 °C for up to 72 h. Two bottles that contained the inoculum supernatant and the medium but no substrates (Inoc_Med) were taken at each time removal point (0 h, 12 h, 18 h and 72 h).

At set incubation times, serum bottles were removed from incubation and plunged into ice water for 20 min. Then 5 mL of this solution was taken for monosaccharide assays. The remainder was stored at -20 °C for freeze-drying followed by proton Nuclear Magnetic Resonance (^{1}H NMR) and Size Exclusion Chromatography (SEC) analysis (see **2.7**).

2.5 ^{1}H NMR and SEC analysis

Before ^{1}H NMR and SEC analyses, the samples were freeze-dried. ^{1}H NMR measurements were performed with a Bruker 500 MHz spectrometer. DMSO-d_6 was used as the solvent for AX analysis, and D_2O was used for XG analysis. Trimethylsilyl propanoic acid sodium salt (TSP) (1.2 mg/mL) in D_2O was added as an internal reference (Lopez-Sanchez, Wang, Zhang, Flanagan, & Gidley, 2016). ^{1}H NMR measurements were run at 353 K to shift the hydrogen-deuterium oxide (HOD) peak upfield away from the anomeric carbohydrate peaks. The ^{1}H NMR signals were assigned based on literature values (Gidley et al., 1991; Hoffmann, Leeflang, de Barse, Kamerling, & Vliegenthart, 1991). The chemical shifts of XG were 5.14 ppm, 4.95 ppm and 4.50-4.63 ppm for galactosylated xylose units, un-substituted xylose units, and β-glycoside units (galactose and glucose) respectively (**supplementary Figure S1**). The chemical shifts of AX were 5.38 ppm, 5.20 ppm, 5.05 ppm and 4.24-4.64 ppm for arabinose mono-linked at C(O)3, mono-linked at C(O)2 or di-linked at C(O)3, di-linked at C(O)2, and xylose units respectively.

For SEC analysis, samples were prepared according to the method described by Feng *et al* (Feng et al., 2018). The samples were analysed according to the methods described by Wang *et al*. (Wang et al., 2015). SEC separates by molecular size, specifically the hydrodynamic radius R_h. The analysis here used linear pullulan standards, and thus the reported molecular R_h is actually not absolute, but that relative to that of pullulan. This has no effect on the inferences from the SEC data.

2.6 Experimental group size and statistical analysis of data

At least two technical replicates were performed for all quantitative assays. The fermentation and the enzymatic hydrolysis of XG and AX were performed using three biological replicates. The error bars in figures represent standard deviations of the mean from biological replicates. SEC data are the means of biological replicates. One-way analysis of variance (ANOVA) was used for significant difference analyses.

The data of cumulative gas production were fitted to the following monophasic model (Groot, Cone, Williams, Debersaques, & Lantinga, 1996) using SAS PROC NLIN (SAS 9.4 for Windows, SAS Institute Inc, Cary, NC, USA, 9.4 Edition 2013):

$$G = A / (1 + (C / t)^{B}) \qquad \text{(Eq. 1)}$$

Where G is the cumulative gas produced at time t (h) and is calculated as mL of gas produced / g DM substrate, A is the asymptotic total gas production, B is the switching characteristic of the curve, and C is the time when half of the asymptotic value has been reached (h).

The maximum rate of the gas production (R_{MAX}) and the time at which it occurs (T_{RMAX}) were calculated according to the equations below (Bauer, Williams, Voigt, Mosenthin, & Verstegen, 2001):

$$T_{RMAX} = C \times [(B\text{-}1) / (B\text{+}1)]^{(1/B)} \quad \text{(Eq. 2)}$$

$$R_{MAX} = A \times B \times C^{B} \times T_{RMAX}^{(-B-1)} / [1 + (C^{B}) \times T_{RMAX}^{(-B)}]^{2} \quad \text{(Eq. 3)}$$

3 Results and discussion

3.1 End-products relate directly or indirectly to substrate degradation

Figure 2 shows the time course of total SCFA, cumulative gas production, and substrate disappearance. Whilst production of total SCFA occurred at the same time that XG or AX levels decreased, gas production increased when almost all the substrates had disappeared. Most of the XG was degraded between 12 h and 18 h and was complete by 24 h, while the maximum rate of gas production occurred at 23 h (T_{RMAX}: 23 h) (**Figure 2a**). The AX disappearance started from ~6 h and finished at 18 h, with the fastest rate of gas production occurring at 19 h (T_{RMAX}: 19 h) (**Figure 2b**). These data are consistent with total SCFA production being related directly to substrate consumption, but indicate that gas was produced at a slower rate, with gas production rate peaking after the substrates were no longer detectable. The faster gas production from AX than XG (P=0.0102) is consistent with the faster disappearance of AX compared with XG. The faster degradation and end product production from AX might be because the structure of AX is less complex than XG, as the latter contains three rather than two sugar types and is more heavily substituted (**Figure 1**). In comparison with our previous study using powdered AX (Feng et al., 2018), the pre-dissolved AX in this study was degraded slower. This might be because the fermentation was carried out under static conditions, substrates in a powdered state might increase local concentration, which facilitates the colonisation of microbes (Macfarlane & Macfarlane, 2006). In addition, in the previous study, although AX was not pre-dissolved, it was mixed (by shaking) and hydrated with the medium overnight. Therefore the accessibility of the substrates to the degrading enzymes might be sufficient for rapid degradation.

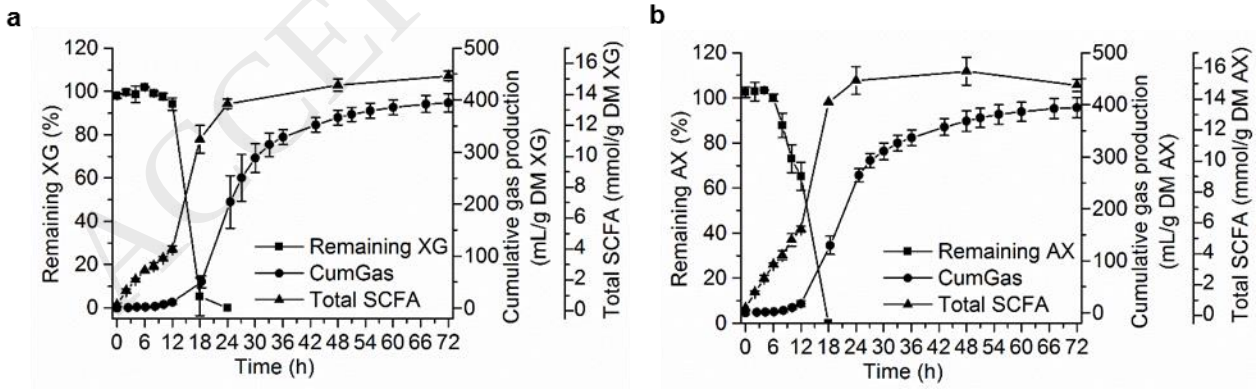

Figure 2: Remaining substrates (measured by ^{1}H NMR) and end product production during the fermentation of xyloglucan (XG: **a**) and arabinoxylan (AX: **b**) with a porcine faecal inoculum. The remaining XG/AX in the culture medium is expressed as the mass percentages compared with the control sample containing the substrate and the medium, but no inoculum.

The end-products of the fermentation of XG and AX show similar profiles, except for slightly more acetate and propionate from AX (**Figure 3a, b**). The amounts of acetate and propionate increased dramatically between 12 h and 18 h, consistent with the rapid depletion of polysaccharides during this period. After the substrates were no longer detectable, acetate increased slowly until 48 h, while propionate increased up to 24 h (**Figure 3**). This shows that the production of these two SCFAs, fuelled by the degradation of the polymers, was faster than the gas production. The production of butyrate increased during the entire fermentation process at an apparently linear rate ($R^2 = 0.95$ for XG and $R^2 = 0.99$ for AX), consistent with butyrate being a secondary metabolite (Duncan et al., 2004) of the fermentation of XG/AX. Gas production (**Figure 2**) also persisted to longer times than acetate or propionate production, again consistent with a contribution from secondary metabolism.

Acetate, propionate and *n*-butyrate are metabolites resulting from carbohydrates being used as an energy source, and are considered beneficial for health (Williams, Verstegen, & Tamminga, 2001). Metabolites resulting from protein fermentation including other SCFA (i.e. *iso*-butyrate, *iso*-valerate and valerate) and ammonia can be used as indicators of protein fermentation, which is considered unfavourable in terms of long-term health outcomes (Williams et al., 2001). The mole percentage of the branched-chain fatty acids to the total fatty acids (BCP) increased in the first six hours (**Figure 3d**), which was the lag phase prior to rapid degradation of the polymers. This suggests that with a lack of fermentation of carbohydrates, the microbes obtained their energy from proteolytic fermentation (Williams et al., 2001). Consistent with this, ammonia (NH_3) also increased during this period (**Figure 3e**). However, during the active fermentation of the polymers (6 – 24 h), BCP and NH_3 decreased, associated with the rapid production of acetate and propionate (**Figure 3 a, b**). After the polymers had disappeared (24 h), BCP and NH_3 increased again. These results support the conclusion that carbohydrates are a preferred energy source, while in the absence of carbohydrate fermentation, amino acids and peptides are more likely to be used as an energy source for microbial growth, resulting in potentially toxic metabolites such as ammonia being produced (Williams et al., 2001).

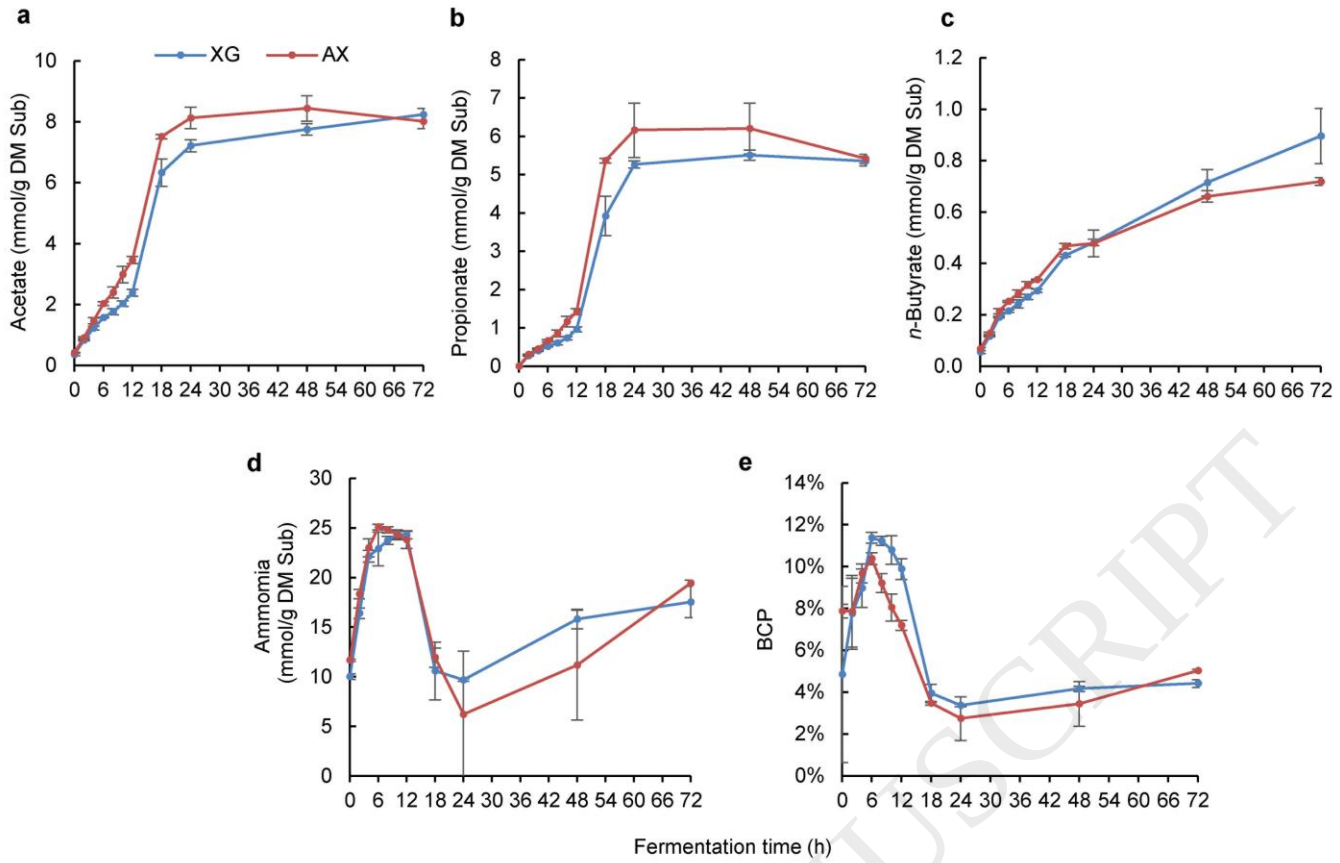

Figure 3 Production of individual short chain fatty acids (**a**: acetate; **b**: propionate; **c**: *n*-butyrate), ammonia (**d**) and the mole percentage of branched-chain fatty acids to total fatty acids (**e**, BCP, includes *iso*-propionate, *iso*-butyrate, *iso*-valerate and valerate) from fermentation of xyloglucan (XG) and arabinoxylan (AX) with a porcine faecal inoculum.

3.2 Depolymerisation initiates XG/AX degradation

Figure 4 shows that at the start of fermentation, the median molecular size of XG (**a**) was about twice that of AX (**b**), and decreased from ~18 nm to ~7 nm at 12 h, though the amount of residual XG did not decrease significantly (**Figure 2a**, $P > 0.05$ between 0 h and 12 h). This smaller molecular size XG was degraded rapidly, and at 18 h, only a small amount of XG (15%) with a molecular size around 2 nm was detected in one of three biological replicates (**Figure 4a**: 18_A*). In the first 6 h, the molecular size of AX decreased from ~9 nm to ~3 nm (**Figure 4b**), though there was no significant loss of AX by NMR (**Figure 2b,** $P > 0.05$ between 0 h and 6 h). At 12 h, the molecular size of AX was further degraded to 2 nm and 39% of AX was degraded during this period (**Figure 2b**). The rest of the residual AX (61%) was completely degraded at 18 h and no molecules with a molecular size bigger than 1 nm were observed by SEC.

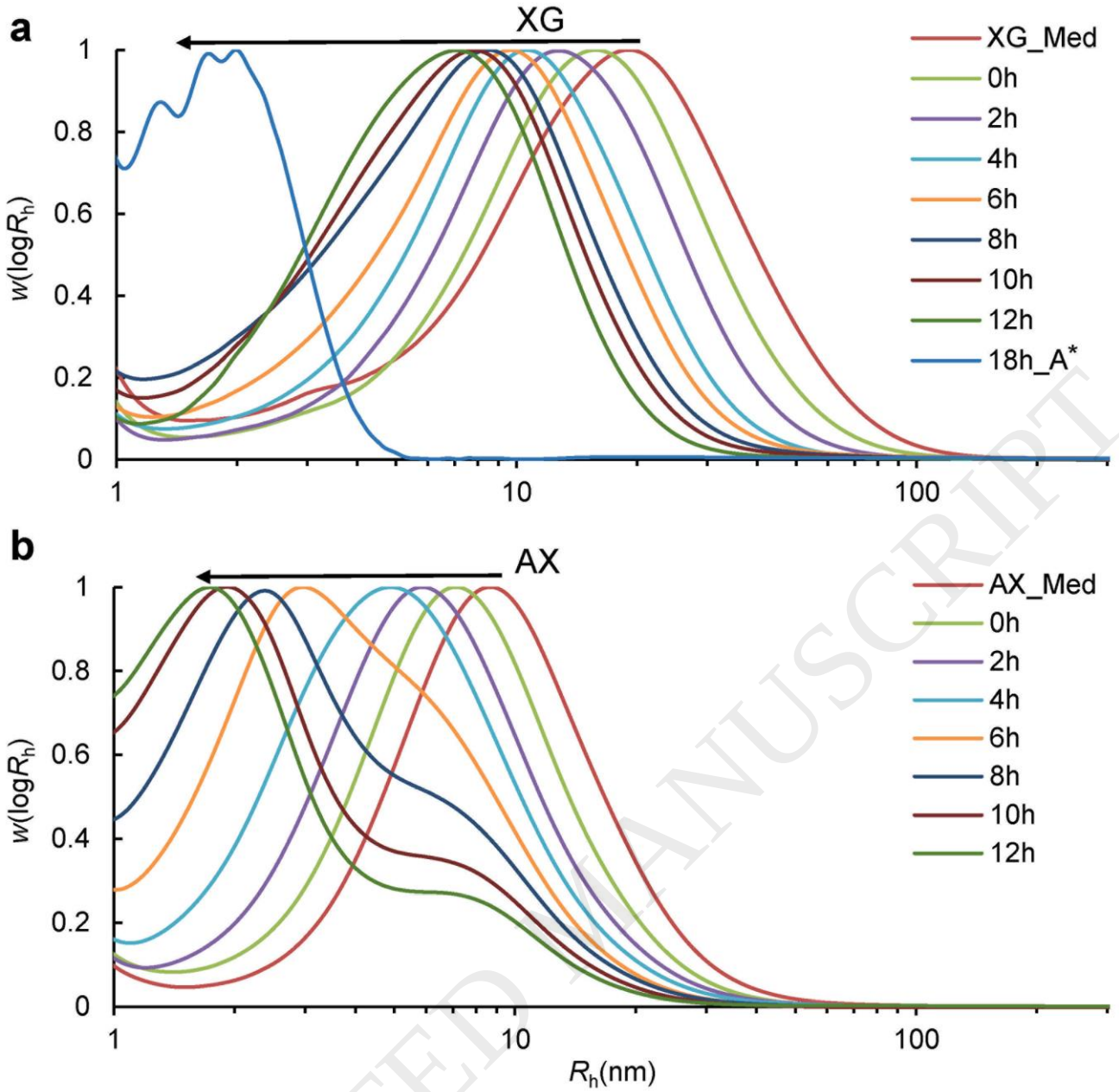

Figure 4 Molecular size distributions (as functions of the relative hydrodynamic radius R_h) of residual xyloglucan (**a**: XG) and arabinoxylan (**b**: AX) during the fermentation. Distributions were normalised to the height of the maximum between 1 and 100 nm. XG_Med and AX_Med were the control samples containing XG/AX and the medium but without the inoculum. *XG was only found in one of three biological replicates.

Though the molecular size decreased in the first twelve hours, ^{1}H NMR results showed no structural changes to the residual XG (**Table 1**). Furthermore, no measurable monosaccharides were detected in the medium during the fermentation of XG (**Supplementary Table S1**), which indicates that depolymerisation of XG was sufficient to initiate the fermentation (Larsbrink, Rogers, et al., 2014; Ravachol et al., 2016). For the one replicate with detectable XG at 18 h (**Table 1**), the ratios of xylose to galactose, glucose to galactose and glucose to xylose increased. This suggests that after XG was depolymerised by *endo*-β-xyloglucanase activity, galactose was the first to be removed by β-galactosidase activity, followed with xylose by α-xylosidase activity. Glucose was the last to be removed by β-glucosidase activity (Harris & Smith, 2006; Larsbrink, Rogers, et al., 2014), as has also proposed for xyloglucan mobilisation in plant (nasturtium) seeds (Crombie, Chengappa, Hellyer, & Reid, 1998).

For AX fermentation, the ratio of mono-linked arabinose at C(O)3 to xylose (A^3/X) decreased from 6 h to 12 h (**Table 1**), indicating extracellular (either secreted or cell-surface located) α-arabinofuranosidase activity targeting arabinoses mono-linked at C(O)3 of the xylan backbone. Arabinoses mono-linked at C(O)2 were not observed for the starting material, but 1% was observed after 4 h, indicating α-arabinofuranosidase action on C(O)3-linked arabinoses of the di-substituents. Arabinofuranosidases encoded by gut symbionts that target the mono-linked arabinoses at C(O)3 and the C(O)3-linked arabinoses of the double substituents have been widely reported (Rogowski et al., 2015; Van Laere et al., 1999). Unlike changes to the proportion of single substitution, the proportion of di-substitution increased during the fermentation, which suggests that microbes preferably utilised mono-linked arabinoses rather than di-linked ones (Pollet et al., 2012). In addition, the A/X ratio also increased during the fermentation, which is different to our previous study, which demonstrated a decreased A/X ratio using AX in a powdered state (Feng et al., 2018). This may be because in the previous study AX was degraded faster (within 8 h) than in this study (within 18 h); the preference of *endo*-xylanases for less-substituted AX is more likely to be noticeable in a slowly fermenting environment. Previous studies examining slowly fermentable AX or AXOS also resulted in an increased A/X ratio (Pastell, Westermann, Meyer, Tuomainen, & Tenkanen, 2009; Pollet et al., 2012).

Change of substitution pattern occurred ca four hours later than the change observed for molecular size by SEC, at which time the latter had decreased from ~9 nm to ~5 nm (**Figure 4b**). This suggests that depolymerisation might also initiate the degradation of AX. However, during the most active fermentation of AX, from 6 h to 18 h, xylan backbone depolymerisation and arabinose release may occur simultaneously, as both the substitution pattern and the molecular size were changed. One consequence of the partial removal of arabinose substituents is that this provides more sites for xylanase to act (Pollet, Delcour, & Courtin, 2010), so arabinose removal and depolymerisation may have acted in concert to reduce the molecular size of AX during the early stages of fermentation.

In comparison with XG, structural changes of AX occurred faster. This might be caused by one or both of two reasons: 1) structural differences between AX and XG; 2) difference in properties between AX and XG degrading enzymes. The molecular size of XG is larger (18 nm vs. 9 nm for AX) and the backbone is more heavily substituted (**Figure 1**) than AX. Hence XG might be more recalcitrant to degradation. In contrast to the possible co-operative action on AX between α-arabinofuranosidases and β-xylanase, *exo*-XG-degrading enzymes are less (or undetectably) active toward polymeric XG (Larsbrink, Rogers, et al., 2014; Larsbrink, Thompson, et al., 2014; Ravachol et al., 2016). In addition, more enzymes are needed to de-branch XG than AX. Therefore, more time might be needed to fully degrade XG.

Table 1 Structural analysis (^{1}H-NMR) of residual xyloglucan (XG) and arabinoxylans (AX) during fermentation.

	XG				AX			
	Gal-	Xyl/Gal	Glc/Gal	Glc/Xyl	A^3/Xyl	A^2/Xyl	A^{2+3}/Xyl	A/X

Sub_Med*	1	2.30^{a}	2.86^{a}	1.24^{a}	0.16^{a}	0.00^{b}	0.15^{d}	0.46^{d}
0h	1	2.32^{a}	2.93^{a}	1.26^{a}	0.16^{a}	0.00^{b}	0.15^{d}	0.46^{d}
2h	1	2.29^{a}	2.86^{a}	1.25^{a}	0.16^{a}	0.00^{b}	0.15^{cd}	0.47^{cd}
4h	1	2.28^{a}	2.85^{a}	1.25^{a}	0.16^{a}	0.01^{a}	0.16^{cd}	0.48^{abc}
6h	1	2.26^{a}	2.84^{a}	1.26^{a}	0.15^{ab}	0.01^{a}	0.16^{bc}	0.48^{bcd}
8h	1	2.26^{a}	2.84^{a}	1.26^{a}	0.14^{bc}	0.01^{a}	0.17^{b}	0.48^{abc}
10h	1	2.28^{a}	2.92^{a}	1.28^{a}	0.12^{cd}	0.01^{a}	0.18^{a}	0.49^{a}
12h	1	2.28^{a}	2.89^{a}	1.27^{a}	0.12^{d}	0.01^{a}	0.18^{a}	0.49^{ab}
18h**	1	2.52	3.33	1.32	–	–	–	–

*Sub_Med is the control sample containing the substrate (XG or AX) and the medium but without the inoculum. Gal-: galactose; Xyl/Gal is the ratio of xylose to galactose; Glc/Gal is the ratio of glucose to galactose; Glc/Xyl is the ratio of glucose to xylose; A^3/Xyl is the ratio of xylose mono-substituted with arabinose at C(O)3 to total xylose; A^2/Xyl is the ratio of xylose mono-substituted with arabinose at C(O)2 to total xylose units; A^{2+3}/Xyl is the ratio of di-substituted xylose units to total xylose units; A/X is the ratio of total arabinose to xylose. **For the fermentation of XG, detectable XG was only found in one of three biological replicates. Differing superscripts (a, b, c, d) in the same column show significant differences ($P < 0.05$).

3.3 Microbial surface degradation of XG/AX releases breakdown products

Two possible mechanisms could account for the changed structures of residual XG/AX in supernatants as analysed with ^{1}H NMR and SEC (**Figure 2, 4**): i) enzymes in the supernatant from the inoculum, or ii) degradation by bacterial surface-located enzymes and subsequent release of enzymatically modified XG/AX into the culture medium. In order to test the former possibility, XG/AX solutions were treated with the inoculum supernatant (containing no microbes) in the same medium and at the same concentration as in the *in vitro* fermentation. SEC results (**Figure 5**) showed that the molecular size decreased, but at a much slower rate than during the fermentation, an effect which was more prominent for AX than XG. This indicated that the activities of soluble depolymerising enzymes in the inoculum supernatant were not enough to account for the structure of residual XG/AX observed during active fermentation. Therefore, at least some XG/AX must have been degraded by bacterial surface-located *endo*-enzymes and the breakdown products released back into the culture medium.

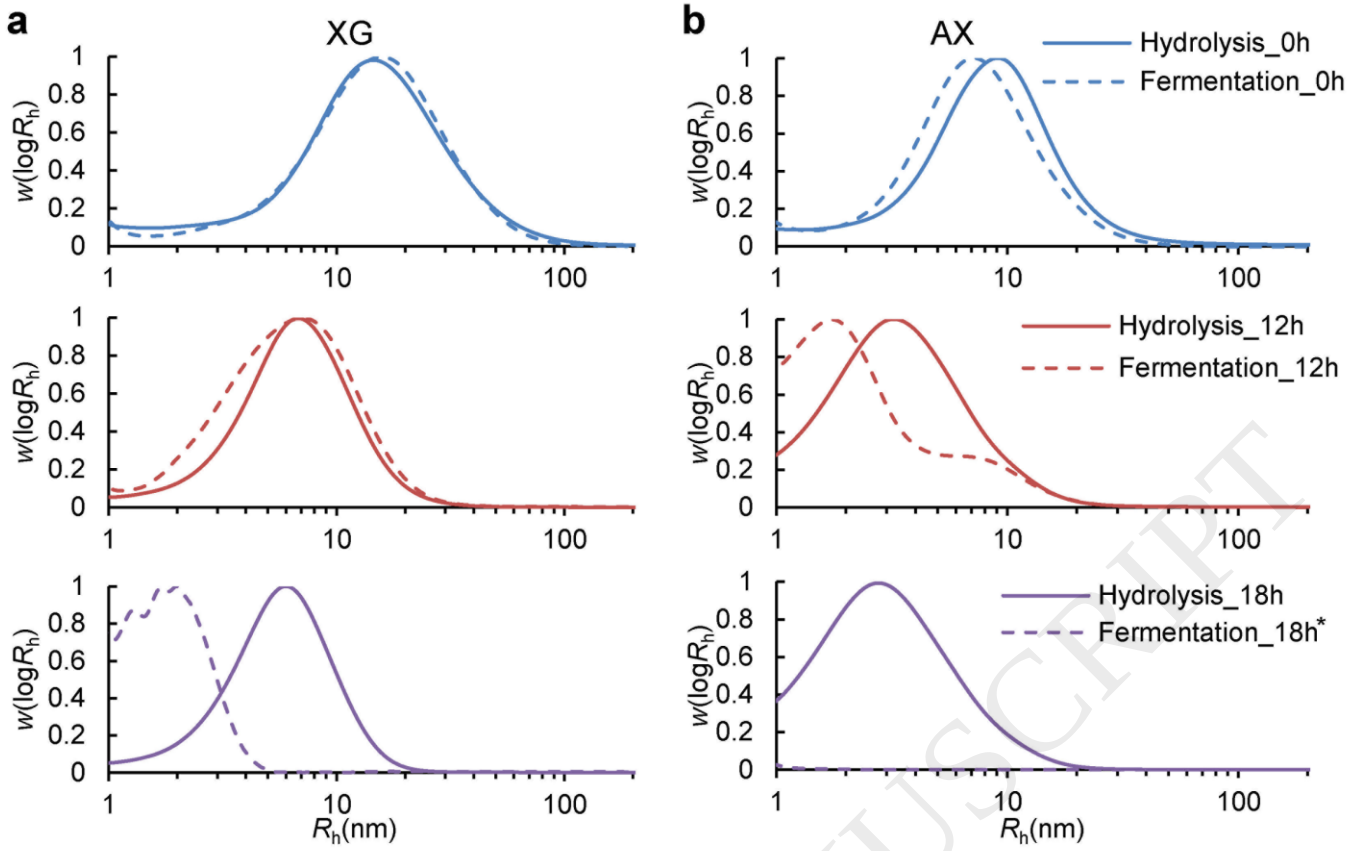

Figure 5 Comparison of molecular size distributions (as functions of the relative hydrodynamic radius R_h) of xyloglucan (XG) and arabinoxylan (AX) hydrolysed by the inoculum supernatant (solid line) and fermented with the whole inoculum (dashed line). Distributions were normalized to the height of the maximum between 1 nm and 100 nm. *For residual AX, the samples were normalised to the height of the maximum from 0.1 nm to 1 nm because no AX larger than 1 nm was detected.

The structures of XG/AX hydrolysed with the inoculum supernatant were further studied using ^{1}H NMR. Small amounts of galactose and xylose (**Supplementary Figure S2**) were detected during the XG incubation, indicating that β-galactosidase and α-xylosidase in the inoculum were active on XG. However, the total monosaccharides released after 72 h accounted for only 1% of the total XG in the solution, and ^{1}H NMR results did not show any change in polymeric sugar ratios (**Table 2**). Therefore, the observed change of sugar ratios in residual XG at 18 h (**Table 1**) during the fermentation could not have been caused by the soluble enzymes in the inoculum, but be due to bacterial surface-located *exo*-degrading enzymes, with the modified XG breakdown products released back into the culture medium.

Compared with XG, the hydrolysis of AX with the inoculum supernatant released more free sugars (**Supplementary Figure S2**), indicating β-xylosidase and α-arabinofuranosidase activity. At 72 h, 21% of AX was hydrolysed accompanied by decreased total A/X, A^3/X and A^{2+3}/X ratios (**Table 2**). The A^{2+3}/X ratio decreased by 0.053 (0.14 × 100% - 0.11 × 79% = 0.053) at 72 h and the A^2/X ratio increased by 0.047 (0.06 × 79% = 0.047). This indicated that α-arabinofuranosidases present in the faecal inoculum hydrolysed the arabinose di-substituents mainly by targeting the C(O)3-linked arabinoses. It has been reported previously that during the fermentation of A^{2+3}XX (α-L-arabinofuranose(Ara*f*)-(1→2)-[α-L-Ara*f*-(1→3)]-β-D-xylopranose(Xyl*p*)-(1→4)-β-D-Xyl*p*-(1→4)-D-Xyl) with a human faecal inoculum, only A^2XX (α-L-Ara*f*-

(1→2)-Xyl*p*-(1→4)-β-D-Xyl*p*-(1→4)-D-Xyl) was observed (Pastell et al., 2009). Therefore, the remaining A^3/X mono-linked arabinoses at C(O)3 were mainly from the substrate, not the product of C(O)2-linked arabinose being cleaved from C(O)2, C(O)3 arabinose di-substituents. At 72 h, the A^3/X ratio was decreased by 0.083 (0.17 × 100% - 0.11 × 79% = 0.083), which was higher than the decreased ratio of A^{2+3}/X (0.053). This implied that the soluble arabinofuranosidases in the inoculum supernatant showed higher activity towards mono-linked arabinoses at C(O)3 than di-linked arabinoses linked at C(O)3. Therefore, the specificities of arabinofuranosidase in the inoculum supernatant were similar to those produced by microbes during the fermentation.

At 12 h, the A^3/X ratio of AX hydrolysed with the inoculum supernatant (**Table 2**) was decreased less than the AX fermented with the whole inoculum (**Table 1**). This difference indicated actions of microbial surface-located *exo*-degrading enzymes, with some of the modified AX released into the medium.

Altogether, the hydrolysis of XG/AX showed that although the pigs were fed on XG/AX-free diets for 10 days before faecal collection, activities of *endo*-β-xyloglucanase, *exo*-β-galactosidase, *exo*-α-xylosidase, *endo*-β-xylanase, *exo*-α-arabinofuranosidases and *exo*-β-xylosidase were present in the inoculum supernatant. However, these activities were not enough to cause the changes observed during fermentation, indicating the actions of microbial surface enzymes and the release of the surface modified products.

Table 2 Structural analysis (^{1}H-NMR) of residual xyloglucan (XG) and arabinoxylan (AX) during hydrolysis with the inoculum supernatant.

Time	XG					AX				
(h)	Gal-	Xyl/Gal	Glc/Gal	Glc/Xyl	Remaining	A^3/Xyl	A^2/Xyl	A^{2+3}/Xyl	A/X	Remaining
0	1	2.29^a	2.90^a	1.27^a	100%^{a}	0.17^a	0.00^c	0.14^a	0.45^a	100%^{a}
12	1	2.28^a	2.92^a	1.28^a	102%^{a}	0.15^b	0.02^b	0.14^a	0.45^a	96%^{a}
18	1	2.27^a	2.89^a	1.28^a	102%^{a}	0.15^b	0.03^b	0.13^a	0.45^a	95%^{a}
72	1	2.27^a	2.90^a	1.28^a	100%^{a}	0.11^c	0.06^a	0.11^b	0.40^b	79%^{b}

Gal-: galactose; Xyl/Gal is the ratio of xylose to galactose; Glc/Gal is the ratio of glucose to galactose; Glc/Xyl is the ratio of glucose to xylose; A^3/Xyl is the ratio of xylose mono-substituted with arabinose at C(O)3 to total xylose; A^2/Xyl is the ratio of xylose mono-substituted with arabinose at C(O)2 to total xylose; A^{2+3}/Xyl is the ratio of di-substituted xylose units to total xylose units; A/X is the ratio of total arabinose to total xylose. The remaining XG/AX is expressed as the mass percentage of substrates remaining during the hydrolysis to the samples at 0 h. Differing superscripts (a, b, c) in the same column show significant differences ($P < 0.05$).

4 Conclusions

During their fermentative utilisation, microbial surface-located enzymes hydrolyse soluble XG and AX, with some breakdown products released back into the culture medium. Structural analyses of residual XG/AX suggested that depolymerisation is a prerequisite for the active fermentation of these polymers, with one consequence being the potential for them to be degraded cooperatively by sharing of the breakdown products. Cross-feeding between different microbes might expand the nutrient availability and result in better microbial growth compared with single microbes (Turroni et al., 2016). In addition, cross-feeding might help to promote a more diverse and healthy microbiota by encouraging the growth of many bacterial species (Turnbaugh et al., 2009). End-product analyses showed high levels of acetate and propionate, and low

percentage of branched-chain fatty acids and ammonia production, indicating the potential benefits of XG/AX fermentation to colonic health. These findings contribute to understanding the principles underpinning the health benefits of dietary fibres. Future studies will investigate the location of XG and AX – degrading enzymes, and the composition and function of the microbial community related with the fermentation of these polymers.

Acknowledgements

This study was supported by the ARC Centre of Excellence in Plant Cell Walls (CE110001007). G.F. was financially supported by China Scholarship Council and the University of Queensland. The authors thank Shiyi Lu, Widaningrum, Alexander Bui, Anja Winkelbach, Mike Passchier, Elena Allefs and Anton Pluschke for their help during the fermentation experiment, and Prof Robert G. Gilbert for his technical support and advice on SEC.

Author contributions

G.F. and M.J.G. conceived the study. G.F., B.M.F., D.M., B.A.W. and M.J.G. designed the experiments. G.F., B.M.F., D.M., B.A.W. and W.Y. performed the experiments. G.F., B.M.F., D.M., B.A.W. and M.J.G. analysed data. G.F. wrote the manuscript and all co-authors edited and agreed to the manuscript content.

References

Amaretti, A., Bernardi, T., Leonardi, A., Raimondi, S., Zanoni, S., & Rossi, M. (2013). Fermentation of xylo-oligosaccharides by *Bifidobacterium adolescentis* DSMZ 18350: kinetics, metabolism, and β-xylosidase activities. *Applied Microbiology and Biotechnology*, 97(7), 3109-3117.

Baethgen, W., & Alley, M. (1989). A manual colorimetric procedure for measuring ammonium nitrogen in soil and plant Kjeldahl digests. *Communications in Soil Science & Plant Analysis*, 20(9-10), 961-969.

Bauer, E., Williams, B., Voigt, C., Mosenthin, R., & Verstegen, M. (2001). Microbial activities of faeces from unweaned and adult pigs, in relation to selected fermentable carbohydrates. *Animal Science*, 73(2), 313-322.

Crombie, H. J., Chengappa, S., Hellyer, A., & Reid, J. S. G. (1998). A xyloglucan oligosaccharide-active, transglycosylating β-D-glucosidase from the cotyledons of nasturtium (*Tropaeolum majus* L) seedlings – purification, properties and characterization of a cDNA clone. *The Plant Journal*, 15(12), 27-38.

Cui, S. W., & Wang, Q. (2009). Cell wall polysaccharides in cereals: chemical structures and functional properties. *Structural Chemistry*, 20(2), 291-297.

Demchick, P., & Koch, A. L. (1995). The permeability of the wall fabric of *Escherichia coli* and *Bacillus subtilis*. *Journal of Bacteriology*, 178, 768-773.

Duncan, S. H., Holtrop, G., Lobley, G. E., Calder, A. G., Stewart, C. S., & Flint, H. J. (2004). Contribution of acetate to butyrate formation by human faecal bacteria. *British Journal of Nutrition*, 91(06), 915-923.

Feng, G., Flanagan, B. M., Mikkelsen, D., Williams, B. A., Yu, W., Gilbert, R. G., & Gidley, M. J. (2018). Mechanisms of utilisation of arabinoxylans by a porcine faecal inoculum: competition and co-operation. *Scientific Reports*, 8(1), 4546.

Gidley, M. J. (2013). Hydrocolloids in the digestive tract and related health implications. *Current Opinion in Colloid & Interface Science*, 18(4), 371-378.

Gidley, M. J., Lillford, P. J., Rowlands, D. W., Lang, P., Dentini, M., Crescenzi, V., . . . Reid, J. G. (1991). Structure and solution properties of tamarind-seed polysaccharide. *Carbohydrate Research*, 214(2), 299-314.

Groot, J. C., Cone, J. W., Williams, B. A., Debersaques, F. M., & Lantinga, E. A. (1996). Multiphasic analysis of gas production kinetics for in vitro fermentation of ruminant feeds. *Animal Feed Science and Technology*, 64(1), 77-89.

Harris, P. J., & Smith, B. G. (2006). Plant cell walls and cell-wall polysaccharides: structures, properties and uses in food products. *International Journal of Food Science & Technology*, 41(s2), 129-143.

Hoffmann, R. A., Leeflang, B. R., de Barse, M. M., Kamerling, J. P., & Vliegenthart, J. F. (1991). Characterisation by 1H-n.m.r. spectroscopy of oligosaccharides, derived from arabinoxylans of white endosperm of wheat, that contain the elements→ 4)[α-L-Ara*f*-(1→3)]-β-D-Xyl*p*-(1→ or→ 4)[α-L-Ara*f*-(1→ 2)][α-L-Ara*f*-(1→ 3)]-β-D-Xyl*p*-(1→. *Carbohydrate Research*, 221(1), 63-81.

Hsieh, Y. S., & Harris, P. J. (2009). Xyloglucans of monocotyledons have diverse structures. *Molecular Plant*, 2(5), 943-965.

Larsbrink, J., Rogers, T. E., Hemsworth, G. R., McKee, L. S., Tauzin, A. S., Spadiut, O., . . . Koropatkin, N. M. (2014). A discrete genetic locus confers xyloglucan metabolism in select human gut Bacteroidetes. *Nature*, 506(7489), 498-502.

Larsbrink, J., Thompson, A. J., Lundqvist, M., Gardner, J. G., Davies, G. J., & Brumer, H. (2014). A complex gene locus enables xyloglucan utilization in the model saprophyte Cellvibrio japonicus. *Molecular Microbiology*, 94(2), 418-433.

Lopez-Sanchez, P., Wang, D., Zhang, Z., Flanagan, B., & Gidley, M. J. (2016). Microstructure and mechanical properties of arabinoxylan and (1, 3; 1, 4)-β-glucan gels produced by cryo-gelation. *Carbohydrate Polymers*, 151, 862-870.

Lowe, S. E., Theodorou, M. K., Trinci, A. P., & Hespell, R. B. (1985). Growth of anaerobic rumen fungi on defined and semi-defined media lacking rumen fluid. *Microbiology*, 131(9), 2225-2229.

Macfarlane, S., & Macfarlane, G. T. (2006). Composition and metabolic activities of bacterial biofilms colonizing food residues in the human gut. *Applied and Environmental Microbiology*, 72(9), 6204-6211.

Mendis, M., Leclerc, E., & Simsek, S. (2016). Arabinoxylans, gut microbiota and immunity. *Carbohydrate Polymers*, 139, 159-166.

Mikkelsen, D., Gidley, M. J., & Williams, B. A. (2011). *In vitro* fermentation of bacterial cellulose composites as model dietary fibers. *Journal of Agricultural and Food Chemistry,* 59(8), 4025-4032.

Miller, E., & Ullrey, D. (1987). The pig as a model for human nutrition. *Annual Review of Nutrition,* 7(1), 361-382.

Neyrinck, A. M., Possemiers, S., Druart, C., Van de Wiele, T., De Backer, F., Cani, P. D., . . . Delzenne, N. M. (2011). Prebiotic effects of wheat arabinoxylan related to the increase in Bifidobacteria, Roseburia and Bacteroides/Prevotella in diet-induced obese mice. *PLoS ONE,* 6(6), e20944.

Pastell, H., Westermann, P., Meyer, A. S., Tuomainen, P. i., & Tenkanen, M. (2009). In vitro fermentation of arabinoxylan-derived carbohydrates by bifidobacteria and mixed fecal microbiota. *Journal of Agricultural and Food Chemistry,* 57(18), 8598-8606.

Pollet, A., Delcour, J. A., & Courtin, C. M. (2010). Structural determinants of the substrate specificities of xylanases from different glycoside hydrolase families. *Critical Reviews in Biotechnology,* 30(3), 176-191.

Pollet, A., Van Craeyveld, V., Van de Wiele, T., Verstraete, W., Delcour, J. A., & Courtin, C. M. (2012). In vitro fermentation of arabinoxylan oligosaccharides and low molecular mass arabinoxylans with different structural properties from wheat (*Triticum aestivum* L.) bran and psyllium (*Plantago ovata* Forsk) seed husk. *Journal of Agricultural and Food Chemistry,* 60(4), 946-954.

Ravachol, J., De Philip, P., Borne, R., Mansuelle, P., Maté, M. J., Perret, S., & Fierobe, H.-P. (2016). Mechanisms involved in xyloglucan catabolism by the cellulosome-producing bacterium *Ruminiclostridium cellulolyticum*. *Scientific Reports,* 6.

Rogowski, A., Briggs, J. A., Mortimer, J. C., Tryfona, T., Terrapon, N., Lowe, E. C., . . . Zheng, H. (2015). Glycan complexity dictates microbial resource allocation in the large intestine. *Nature Communications,* 6.

Roura, E., Koopmans, S.-J., Lallès, J.-P., Le Huerou-Luron, I., de Jager, N., Schuurman, T., & Val-Laillet, D. (2016). Critical review evaluating the pig as a model for human nutritional physiology. *Nutrition research reviews*, 1-31.

Schultink, A., Liu, L., Zhu, L., Pauly, M. (2014). Structural Diversity and Function of Xyloglucan Sidechain Substituents. *Plants*, 3, 526-542.

Turnbaugh, P. J., Hamady, M., Yatsunenko, T., Cantarel, B. L., Duncan, A., Ley, R. E., . . . Affourtit, J. P. (2009). A core gut microbiome in obese and lean twins. *Nature,* 457(7228), 480-484.

Turroni, F., Milani, C., Duranti, S., Mancabelli, L., Mangifesta, M., Viappiani, A., . . . Ferrarini, A. (2016). Deciphering bifidobacterial-mediated metabolic interactions and their impact on gut microbiota by a multi-omics approach. *The ISME Journal,* 10(7), 1656.

Van Laere, K., Voragen, C., Kroef, T., Van den Broek, L., Beldman, G., & Voragen, A. (1999). Purification and mode of action of two different arabinoxylan arabinofuranohydrolases from *Bifidobacterium adolescentis* DSM 20083. *Applied Microbiology and Biotechnology,* 51(5), 606-613.

Wang, K., Wambugu, P. W., Zhang, B., Wu, A. C., Henry, R. J., & Gilbert, R. G. (2015). The biosynthesis, structure and gelatinization properties of starches from wild and cultivated African rice species (*Oryza barthii* and *Oryza glaberrima*). *Carbohydrate Polymers,* 129, 92-100.

Williams, B. A., Bosch, M. W., Boer, H., Verstegen, M. W., & Tamminga, S. (2005). An in vitro batch culture method to assess potential fermentability of feed ingredients for monogastric diets. *Animal Feed Science and Technology,* 123, 445-462.

Williams, B. A., Mikkelsen, D., Le Paih, L., & Gidley, M. J. (2011). In vitro fermentation kinetics and end-products of cereal arabinoxylans and (1, 3; 1, 4)-β-glucans by porcine faeces. *Journal of Cereal Science,* 53(1), 53-58.

Williams, B. A., Verstegen, M. W., & Tamminga, S. (2001). Fermentation in the large intestine of single-stomached animals and its relationship to animal health. *Nutrition research reviews,* 14(02), 207-228.

Yamatoya, K., Shirakawa, M., Kuwano, K., Suzuki, J., & Mitamura, T. (1996). Effects of hydrolyzed xyloglucan on lipid metabolism in rats. *Food Hydrocolloids,* 10(3), 369-372.